Nonlinear dynamical motion of cellular structures in the cochlea

Conor Heneghan and Malvin C. Teich

Columbia University,
Departments of Electrical Engineering and Applied Physics,
New York, NY 10027, USA

Shyam M. Khanna

Columbia College of Physicians & Surgeons,
Department of Otolaryngology,
New York, NY 10032, USA

Mats Ulfendahl

Karolinska Institutet,
Department of Physiology II,
S-104 01 Stockholm, Sweden

ABSTRACT

The time course of the velocity of vibration was measured in individual sensory cells (outer hair cells and Hensen's cells from the third and fourth turns of a guinea-pig temporal-bone preparation) for a variety of applied acoustic stimuli. The methods of preparation and interferometric measurement have been described earlier. To observe the cell's response for a continuous and large range of acoustic intensities, an amplitude modulated (AM) tone with fixed modulation characteristics and a wide range of carrier frequencies f_c was used. The peak acoustic intensities of the applied tones were in excess of 90 dB:re .0002 dynes/cm^2. A spectrogram was used to analyze the velocity response of the cell. This is a three-dimensional representation that exhibits the time evolution of the amplitudes of all of the spectral components in the response. In the fourth turn of the cochlea, where cells responding to the lowest acoustic frequencies are located, AM tones with carrier frequencies below the characteristic frequency (CF) of the cell (the frequency of maximal vibratory response) gave responses with multiple harmonic components, with the largest component occurring at a frequency close to the CF of the cell. For carrier frequencies near the CF, multiple harmonic components were also present, with odd harmonic components ($3f_c$, $5f_c$, etc.) higher in magnitude than even harmonic components ($2f_c$, $4f_c$, etc.). For carrier frequencies above the CF, fewer harmonic components were present and they were of smaller magnitude. In the third turn, qualitatively similar results were found. An additional feature seen in the third turn recordings was the presence of half-harmonic spectral components ($f_c/2$, $3f_c/2$, $5f_c/2$, etc.) in the response to stimuli with carrier frequencies near and above the CF. The emergence of spectral components with these types of patterns is consistent with a class of nonlinear oscillator models that can be driven into chaotic regimes. One example is the behavior of the velocity $\dot{x}(t)$ in a generalized driven Duffing oscillator, for which the equation of motion takes the form $\ddot{x}(t) + \alpha\dot{x}(t) - \beta x(t) + \gamma x^3(t) = F(t)$, where α, β, and γ are constants and the forcing function $F(t)$ is a slowly modulated AM tone.

1. INTRODUCTION

1.1. Overview of the hearing process in the mammalian auditory system

Sound is received by the pinna (external ear) and travels through the ear canal to the tympanic membrane. The middle ear converts this acoustic signal into mechanical vibrations of the ossicular chain. These vibrations are transmitted, via the footplate of the stapes, to the fluid-filled inner ear[1,2,3]. Fluid vibrations result in mechanical

vibrations of the basilar membrane and the sensory cells supported by it in the organ of Corti. The organ of Corti, which contains many types of cells, is located within the cochlea, a bony fluid-filled snail-like structure. Of these cells, the inner and outer hair cells are most directly associated with the auditory transduction process.

Within the cochlea there is a tonotopic mapping — that is, cells at a particular location respond most vigorously to certain frequencies. At the base (first turn) of the cochlea, near where the vibrations are transmitted through the oval window, the vibratory response of the cells reflects mechanical tuning at high acoustic frequencies (in the 30 kHz region in the guinea-pig). In the higher turns of the cochlea (there are four turns in the guinea-pig cochlea), the tuning of the cells' responses occurs at successively lower and lower frequencies. In the third turn of the guinea-pig cochlea, the cells respond maximally to frequencies in the range 500 - 900 Hz, whereas in the fourth turn, the maximum response occurs for frequencies below about 500 Hz. The frequency at which a cell displays its maximum mechanical response is termed the characteristic frequency (CF) of that cell.

It is well known that nonlinearities are present in the cochlear transduction process, and their behavior has been investigated by researchers in various species of animal[4,5,6,7]. The determination of whether these nonlinearities play a significant role in the functioning of the cochlea, and their precise locations are topics of current research. This paper focuses on characterizing the nonlinear velocity responses of two types of sensory cells in the third and fourth turn of the guinea-pig temporal-bone preparation[8,9] by considering the spectral content of their responses as a function of time.

1.2. Experimental description

We have measured the vibratory motion of outer hair cells and Hensen's cells at the reticular lamina in response to various acoustic stimuli, using heterodyne interferometry[8]. Hensen's cells are mechanically tightly coupled to the third row of outer hair cells. Hensen's cells have a much higher optical reflectivity than outer hair cells, and therefore their vibrations can be measured with greater signal-to-noise ratio. Measurements were carried out in the third and fourth turns of the guinea-pig temporal-bone preparation described by Ulfendahl *et al.*[9]. In this preparation, the left temporal bone, containing the cochlea, is removed intact from a freshly sacrificed animal. The cochlea and its associated structures are maintained in a viable state for periods of several hours, by immersion in a specially prepared and oxygenated tissue-culture medium.

The cochlea is stimulated acoustically through the intact auditory canal. To prevent the tympanic membrane from drying and cracking, the middle ear is also immersed in tissue culture medium whereas under normal physiological conditions, it is air-filled. This introduces an acoustical loss of approximately 30 dB[10]. The acoustic sound pressure levels quoted in this paper have been adjusted for this loss by subtracting 30 dB from the sound pressure levels measured at the tympanic membrane. Sound pressure levels were measured simultaneously with the cellular velocity recordings, using a probe microphone placed near the tympanic membrane.

The details of the measuring and stimulus generation techniques have been fully described elsewhere[8]. This paper concentrates on the analysis of the velocity response of these cells to amplitude modulated (AM) tones. These stimuli are ideally suited for investigating the nonlinear dynamical behavior as this particular choice of stimulus has fixed frequency but a slowly varying input level. It allows us to observe, in a single experiment, the cell's response for a continuous and large range of acoustic intensities. The AM tone is, however, a nonstationary stimulus over the time scale of the experimental recordings so that a proper representation of the response in the spectral domain must be used. Accordingly, we use the spectrogram, which is a suitable time-frequency representation for capturing the time-varying spectral character of the cellular velocity responses.

2. ANALYSIS TECHNIQUES

2.1. The Short-Time Fourier Transform and spectrogram

A commonly used time-frequency representation[11,12] is the spectrogram (*SPEC*), which is defined as:

$$SPEC_x^g(t,f) = |STFT_x^g(t,f)|^2 \tag{1}$$

with the Short-Time Fourier Transform (*STFT*) defined as:

$$STFT_x^g(t,f) = \int_{-\infty}^{\infty} [x(u)g^*(u-t)] \exp(-j2\pi fu)\ du, \tag{2}$$

where $x(t)$ represents the time waveform being analyzed, $g(t)$ represents a window function in time, t is the time variable, and f is the frequency variable. A Gaussian window $[g(t) = \exp(-t^2)]$ provides a reasonable choice for the window function, since it minimizes the time-frequency uncertainty product[11]. Once a window length L is chosen, the time-frequency uncertainty product is fixed — a good rule of thumb is to choose the window length so that the signal appears 'relatively stationary' within the window. In our case a window length $L = 128$ samples was appropiate. This corresponds to 25.6 ms at the 5 kHz sampling rate used in recording our data.

We have chosen to plot simply the magnitude of the *STFT*, rather than its square, in our figures. This choice of format affords us the ability to show both high and low magnitude components more effectively on the same plot, for our particular class of signals. However as the spectrogram is a term often used to refer to both the magnitude of the *STFT* and its square (which is the strict definition of the spectrogram), we will refer to the magnitude of the *STFT* as the spectrogram, in the remainder of this paper.

A sampled version of the spectrogram was calculated using a summation approximation of (2):

$$STFT[n,k] = \sum_{m=0}^{L-1} x[n+m]w[m] \exp\left(\frac{-j2\pi mk}{N}\right), \quad 0 \le k \le N-1, \tag{3}$$

where n is the discrete time index, k is the discrete frequency index, and $w[n]$ represents the Gaussian window sampled in the range $[-2,2]$:

$$w[n] = \exp\left[\left(-2 + \frac{4n}{L-1}\right)^2\right], \quad 0 \le n \le L-1. \tag{4}$$

The value of N (which sets the number of discrete frequencies at which the *STFT* is sampled in the frequency domain) was chosen equal to L. The spectrogram was not evaluated for all values of n; sampling at values of n that were multiples of 32 gives a sufficiently detailed picture of the spectrogram for our purposes. This is equivalent to saying that the window is moved through 32 time samples for successive evaluations of the *STFT*.

In our figures we present the spectrogram in a three dimensional visual format, often referred to as a 3-D spectral plot. In this format, time and frequency form the bottom plane, and *STFT* magnitude is represented on a linear axis in the third dimension.

3. RESULTS

3.1. Stimulus characteristics

To examine the frequency-dependent nature of the velocity response of sensory cells in the cochlea we applied 100%-modulated AM stimuli with a fixed modulation frequency (2.44 Hz), varying the carrier frequency of the

stimulus. This allowed us to examine the variable nature of the nonlinear velocity response of a given cell as the carrier frequency was altered from below to above the CF. Here, we detail the responses of two cells, a fourth turn Hensen's cell and a third turn outer hair cell, from two different preparations. The sampling frequency was fixed at 5 kHz in all cases.

3.2. Response of a fourth turn Hensen's cell to AM stimuli

In Figs. 1, 2, and 3 we show the response recorded at a Hensen's cell located in the fourth turn of the guinea-pig cochlea. This cell has a characteristic frequency of approximately 220 Hz. Figure 1 shows the response of this cell when an AM tone with a carrier frequency f_c = 97 Hz (below CF) is applied to the cochlear preparation. In Fig. 1(a), we see the overall velocity response of the cell over one cycle of the modulation envelope. The response does not follow the shape of the input envelope; it is distorted and asymmetrical about the zero of velocity. Figure 1(b) shows in detail the velocity response from the central portion of the modulation envelope, in the time range 0.18 - 0.22 s. The spectrogram of the velocity response [Fig. 1(c)] shows the time behavior of the spectral content in the velocity time waveform. The spectrogram reveals the presence of many spectral components, whose frequencies are all multiples of the carrier frequency. The component at f_c is the first to appear in time, but near the center of the envelope the spectral component at $2f_c$ matches the magnitude of the f_c component. It should be noted, however, that $2f_c$ (= 194 Hz) is closer to CF than f_c itself, so it is not that surprising that this tuned system vibrates maximally at the frequency component closest to its favored frequency. In addition, the spectrogram shows that the spectral components at $4f_c$ and $6f_c$ are greater than the odd harmonic components at $3f_c$ and $5f_c$. All spectral components are seen to follow the time course of the input envelope quite well.

Figure 2 shows the response of this cell when an AM tone with a carrier frequency f_c = 220 Hz (at CF) is applied to the cochlear preparation. In Fig. 2(a), we see the overall velocity response of the cell over one cycle of the modulation envelope. The response does not follow the shape of the input envelope, and its magnitude is greater than the response shown in Fig. 1(a), since we are at the CF of the cell. Figure 2(b) shows in detail the velocity response from the central portion of the modulation envelope, in the time range 0.18 - 0.22 s. The spectrogram of the velocity response [Fig. 2(c)] shows the presence of multiple spectral components in the velocity response, as in Fig. 1(c). The component at f_c is first to appear in time, followed closely in time by the component at $2f_c$ and, then by the higher harmonics. However the component at $2f_c$ is quickly surpassed in magnitude by the odd harmonic components at $3f_c$, $5f_c$, and $7f_c$. Each spectral component follows the input envelope quite smoothly in time.

Figure 3 shows the response of this cell when an AM tone with a carrier frequency f_c = 439 Hz (above CF) is applied to the cochlear preparation. In Fig. 3(a), we see the overall velocity response of the cell over one cycle of the modulation envelope. The response follows the shape of the input envelope reasonably well, though there is some asymmetry towards positive velocities. Fig. 3(b) shows in detail the velocity response at the center of the modulation envelope, in the time range 0.18 - 0.22 s. The spectrogram of the velocity response [Fig. 3(c)] shows that three principal spectral components are present. The component at f_c is dominant and follows the shape of the input envelope. The components at $2f_c$ and $3f_c$ are far smaller in magnitude and only appear at the highest stimulus levels near the center of the input waveform. There is also a component at $4f_c$ which is just barely visible. In Fig. 3(c), we can also discern a low-amplitude steady component at a frequency just below 200 Hz, which continues at approximately the same level before the onset of, and throughout the time-course of, the AM stimulus. The behavior of this component is reminiscent of the spontaneous cellular vibrations previously observed in some third turn Hensen's cells, both in the absence of a stimulus[13,14] and in its presence[15].

3.3. Response of a third turn outer hair cell to AM stimuli

In Figs. 4, 5, and 6 we show the response recorded at an outer hair cell located in the third turn of the guinea-pig cochlea. Similar third turn data has been reported previously[16,17,18]. This cell has a characteristic frequency of approximately 750 Hz. Figure 4 shows the response of this cell when an AM tone with a carrier frequency f_c = 390 Hz (below CF) is applied to the cochlear preparation. In Fig. 4(a), we see the overall velocity response of the cell over one cycle of the modulation envelope. The response follows the shape of the input envelope quite well. Figure 4(b) shows in detail the velocity response from the central region of the modulation envelope in the time range 0.18

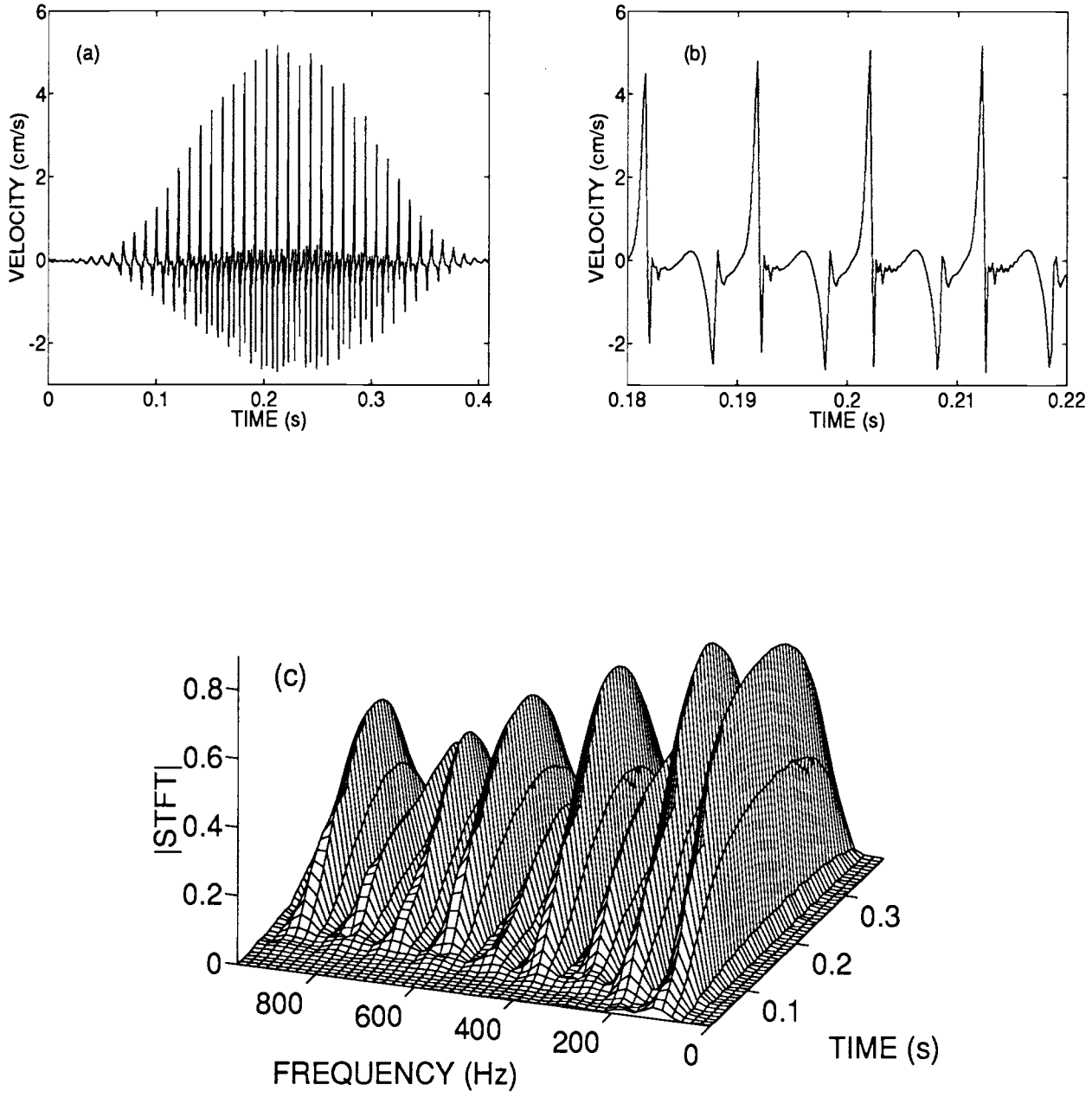

Figure 1: Velocity response of a Hensen's cell (34231238.wv1) in the fourth turn of a guinea-pig temporal-bone preparation to an AM stimulus with a carrier frequency of 97 Hz (below CF) and a modulation frequency of 2.44 Hz. The highest sound pressure level, occurring at the center of the input envelope, was 96 dB:re .0002 dynes/cm^2. (a) Time waveform of the velocity response (in cm/s) of the cell. Note the asymmetry between positive and negative velocities. (b) Detailed view of the time waveform in the central region of the input envelope (from 0.18 s to 0.22 s). The waveform shape, while unusual, is reasonably repeatable over the four cycles shown. (c) Spectrogram of the velocity response shown in (a). The x and y axes represent time (s) and frequency (Hz) respectively, and spectral magnitude is plotted on the z axis (unitless). The spectrogram shows spectral components at the carrier frequency f_c, and at higher harmonic frequencies. The component at $2f_c$ is approximately equal to the component at f_c.

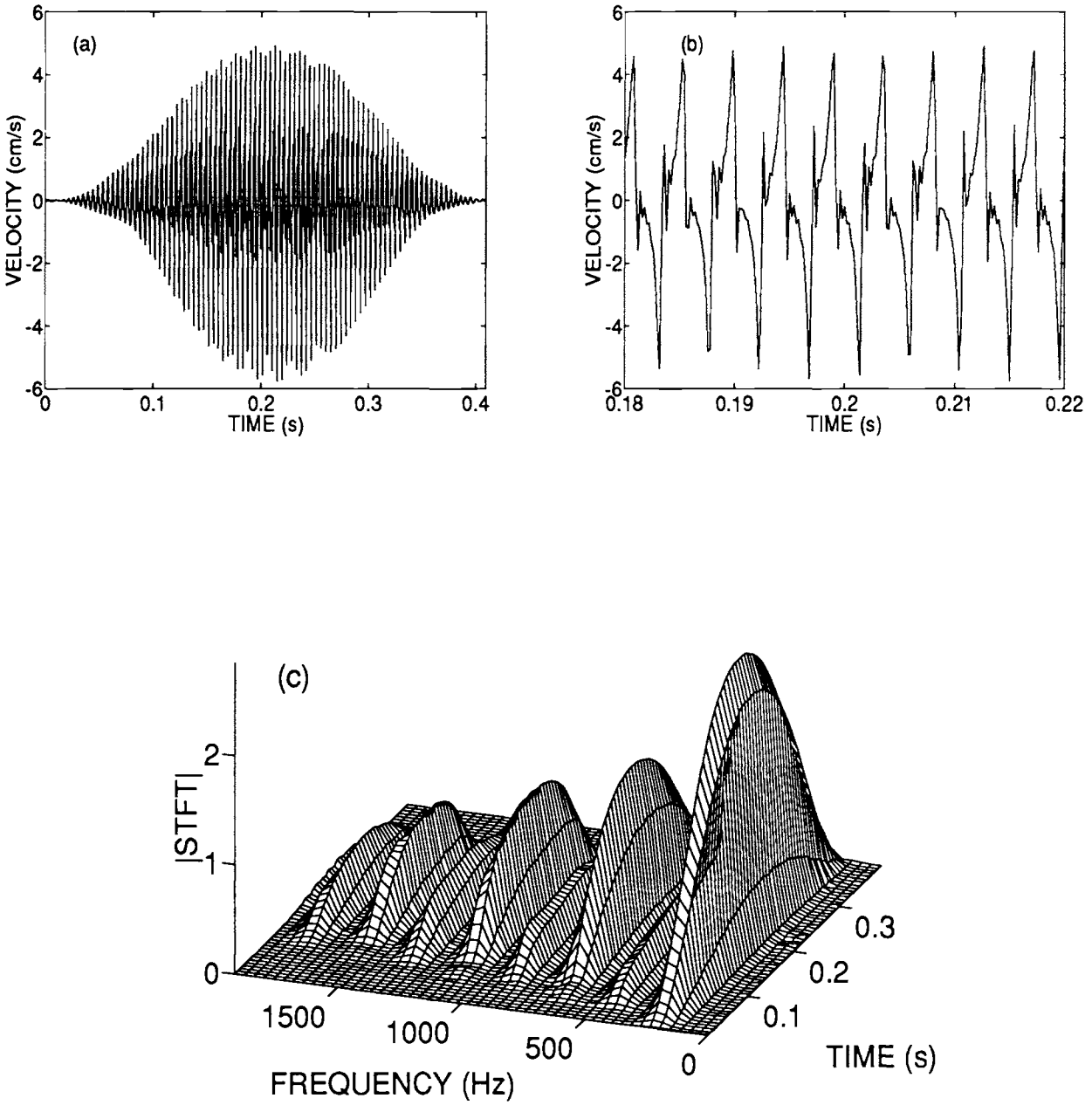

Figure 2: Velocity response of the same Hensen's cell as in Fig. 1, but now to an AM stimulus with a carrier frequency of 220 Hz (at CF) and a modulation frequency of 2.44 Hz. The highest sound pressure level, occurring at the center of the input envelope, was 94 dB:re .0002 dynes/cm^2. (a) Time waveform of the velocity response (in cm/s) of the cell. The time waveform more closely follows the envelope of the stimulus than that shown in Fig. 1. (b) Detailed view of the time waveform in the central region of the input envelope (from 0.18 s to 0.22 s). The waveform shape is reasonably repeatable over the nine cycles shown. (c) Spectrogram of the velocity response shown in (a). The spectrogram shows spectral components at the carrier frequency f_c, and at higher harmonic frequencies. The odd harmonic components at $3f_c$, $5f_c$, and $7f_c$ are larger in magnitude than the even harmonics directly below them in frequency (i.e., $2f_c$, $4f_c$, and $6f_c$, respectively). All spectral components follow the envelope of the input stimulus reasonably well.

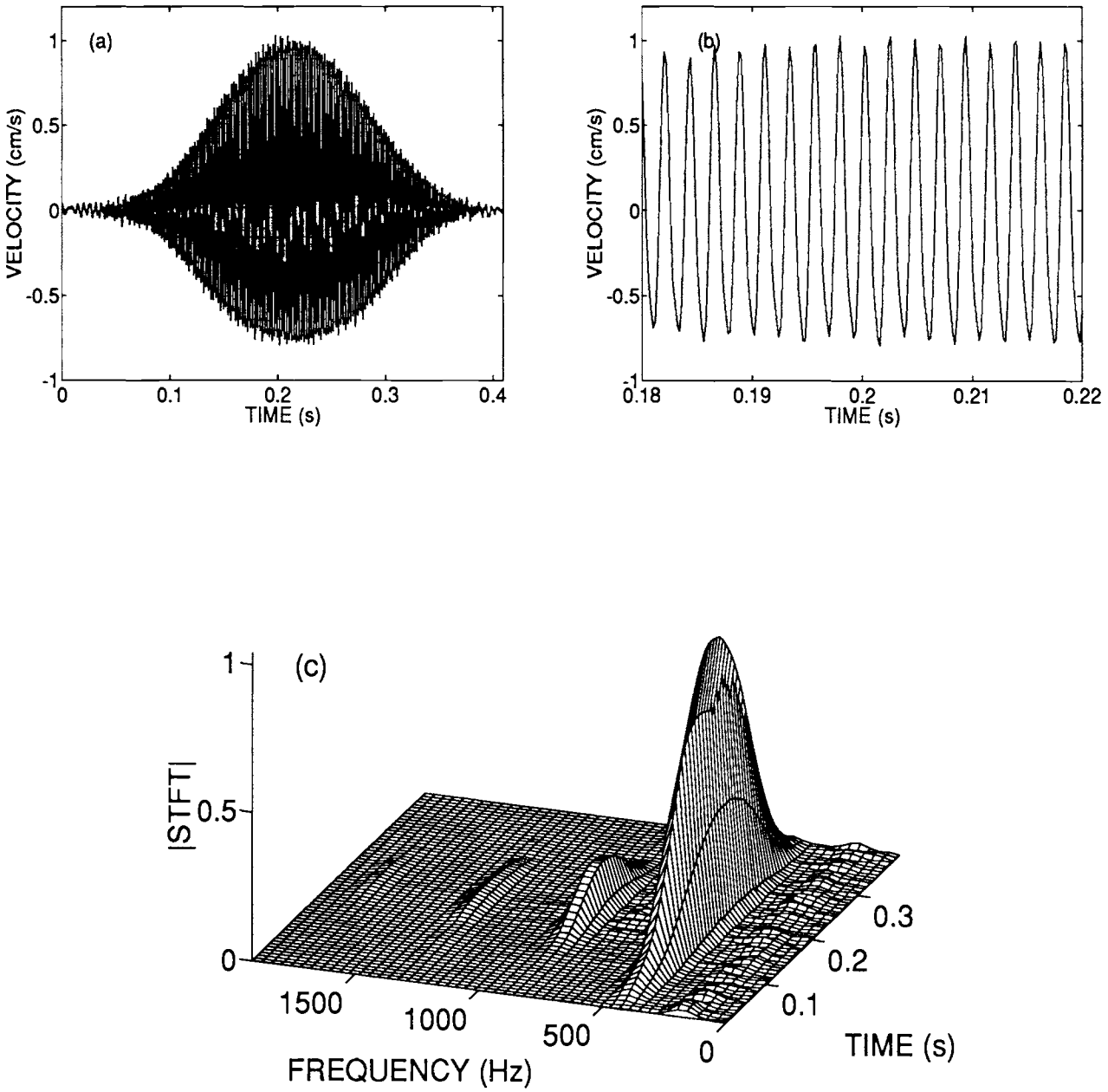

Figure 3: Velocity response of the same Hensen's cell as in Figs. 1 and 2, but now to an AM stimulus with a carrier frequency of 439 Hz (above CF) and a modulation frequency of 2.44 Hz. The highest sound pressure level, occurring at the center of the input envelope, was 94 dB:re .0002 dynes/cm^2. (a) Time waveform of the velocity response (in cm/s) of the cell. The time waveform follows the envelope of the stimulus quite well. (b) Detailed view of the time waveform in the central region of the input envelope (from 0.18 s to 0.22 s). (c) Spectrogram of the velocity response shown in (a). The spectrogram shows spectral components at the carrier frequency f_c, and at three harmonic frequencies, $2f_c$, $3f_c$ and $4f_c$. (The component at $4f_c$ is barely visible). The dominant spectral component is clearly that at the carrier frequency.

- 0.22 s. The spectrogram of the velocity response [Fig. 4(c)] shows that many harmonic components are present in the response, though the component at the carrier frequency clearly dominates. The odd harmonic components (at $3f_c$ and $5f_c$) are slightly larger in magnitude than the components at $2f_c$ and $4f_c$ [compare with Fig. 2(c)].

Figure 5 shows the response of this cell when an AM tone with a carrier frequency f_c = 756 Hz (at CF) was applied to the cochlear preparation. In Fig. 5(a), we see the overall velocity response of the cell over one cycle of the modulation envelope. The response does not follow the shape of the input envelope, and there appears to be a distinct velocity (approximately 0.3 cm/s) at which the response 'breaks up' into a more complex response waveform (see arrow on diagram). Fig. 5(b) shows in detail the velocity response from the central region of the modulation envelope in the time range 0.18 - 0.22 s. The spectrogram of the velocity response [Fig. 5(c)] shows some rather unique features that are significantly different from the responses presented above, i.e., the presence of spectral components at the half-harmonic frequencies $f_c/2$, $3f_c/2$, and $5f_c/2$. These components, which have been observed previously[19,20], occur near the center of the envelope but do not follow it in time. In fact, the appearance of these half-harmonic components is sporadic and not seemingly related in any direct way to the input stimulus envelope. Moreover, at the center of the response waveform (in the range 0.15 - 0.25 s approximately), there is a spectral broadening of the response, i.e., energy is present at frequencies unrelated to the carrier frequency. This raising of the 'noise-floor' is reminiscent of the transition from a quasi-periodic to a noise-like spectrum in the response of a driven chaotic system[21].

Figure 6 shows the response of this cell when an AM tone with a carrier frequency f_c = 961 Hz (above CF) was applied to the cochlear preparation. In Fig. 6(a), we see the overall velocity response of the cell to one cycle of the modulation envelope. The response follows the shape of the input envelope reasonably well, apart from the distinct notch in the waveform at 0.15 s. Fig. 6(b) shows in detail the velocity response from the central region of the modulation envelope, in the time range 0.18 - 0.22 s. The spectrogram of the velocity response [Fig. 6(c)] shows that the component at the carrier frequency has by far the largest amplitude, with a small spectral component also present at $2f_c$. The half-harmonic components ($f_c/2$, $3f_c/2$, and $5f_c/2$) seen in Fig. 5(c) are still present in the response, but they are barely visible. As in the fourth turn, the response for carrier frequencies above CF is dominated by the f_c component, even if the carrier frequency is only slightly greater than CF.

4. DISCUSSION

4.1. Frequency dependence of the nonlinearity in the velocity response of cochlear sensory cells

The application of a slowly varying AM stimulus to various cells in the guinea-pig temporal-bone preparation has allowed us to discern some general patterns of behavior in the velocity responses of these cells. The results we have presented in Section 3 are typical of the recordings we have observed from 41 data sets, taken from outer hair cells and Hensen's cells in both the third and fourth turns of the guinea-pig cochlea. Analysis of the velocity response waveforms using the spectrogram has shown the following:

- For carrier frequencies below the CF, multiple harmonic components are present in the response waveform. For the fourth turn measurements we have seen a tendency for the harmonic component nearest the CF to become dominant, particularly for stimuli with high peak intensity. In the third turn measurements, with f_c below the CF, we also see multiple harmonic components, but the component at the carrier frequency is generally the largest in magnitude.
- For carrier frequencies near the CF, odd harmonic components dominate their neighboring even harmonics. In the third turn, we have seen numerous examples of the appearance of half-harmonic components and a broadening of the spectral response for very high peak acoustic intensities, for both outer hair cells and Hensen's cells. In the fourth turn, we have not yet seen evidence for the presence of half-harmonic spectral components or spectral broadening.
- For carrier frequencies above the CF, the spectral component at the carrier frequency is dominant in magnitude for both third and fourth turn cells. There may be other harmonic components. They are, however, small in magnitude in comparison with the component at the carrier frequency.

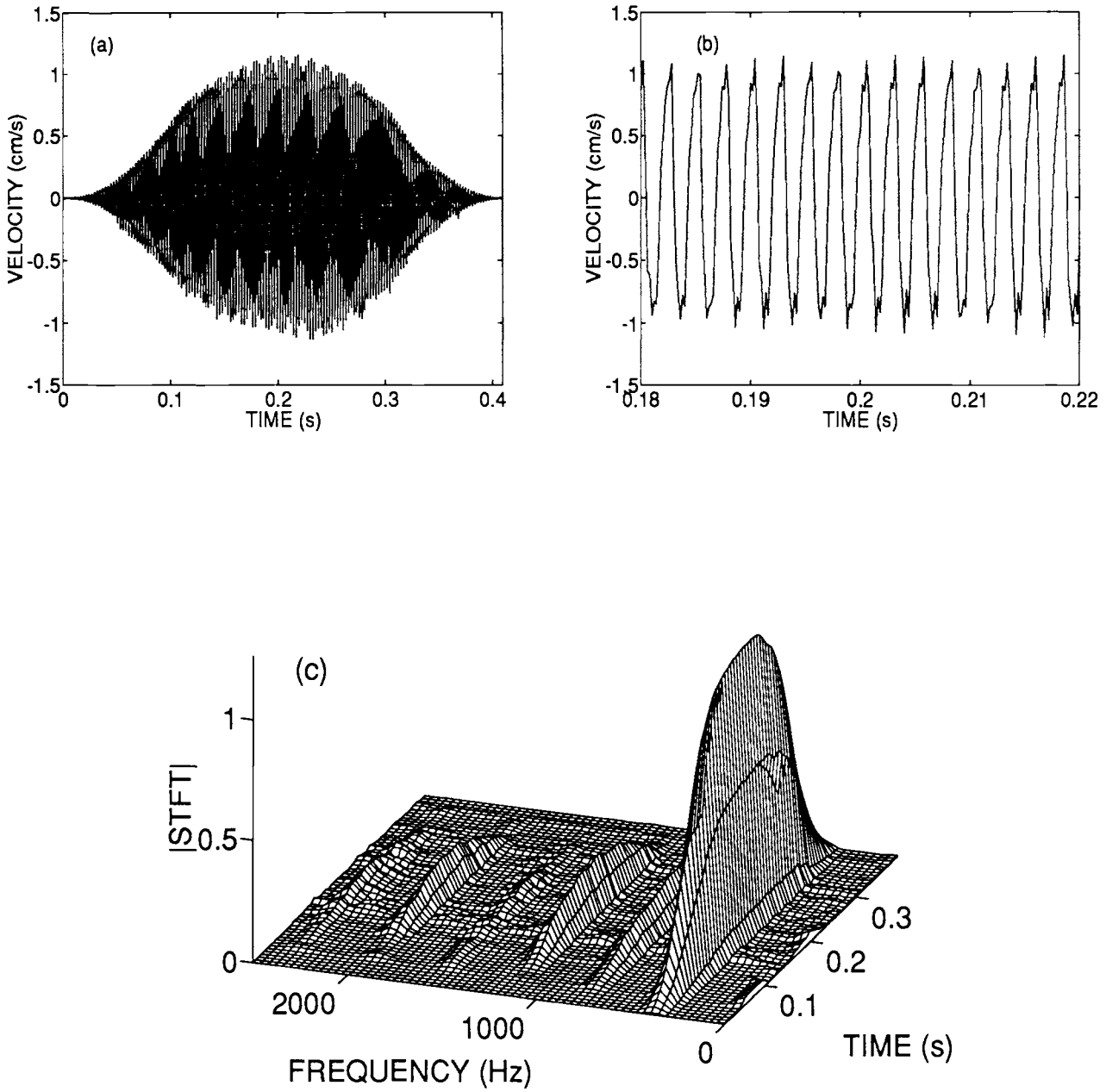

Figure 4: Velocity response of an outer hair cell (0a181442.wv3) in the third turn of a guinea-pig temporal-bone preparation to an AM stimulus with a carrier frequency of 390 Hz (below CF) and a modulation frequency of 2.44 Hz. The highest sound pressure level, occurring at the center of the input envelope, was 95 dB:re .0002 dynes/cm^2. (a) Time waveform of the velocity response (in cm/s) of the cell. (b) Detailed view of the time waveform in the central region of the input envelope (from 0.18 s to 0.22 s). The small notches on the waveform occurring near each peak are evidence of the presence of higher frequency components. (c) Spectrogram of the velocity response shown in (a). The spectrogram shows spectral components at the carrier frequency f_c, and at five higher harmonic frequencies. The components at $3f_c$ and $5f_c$ are greater in magnitude than the components at $2f_c$ and $4f_c$, respectively.

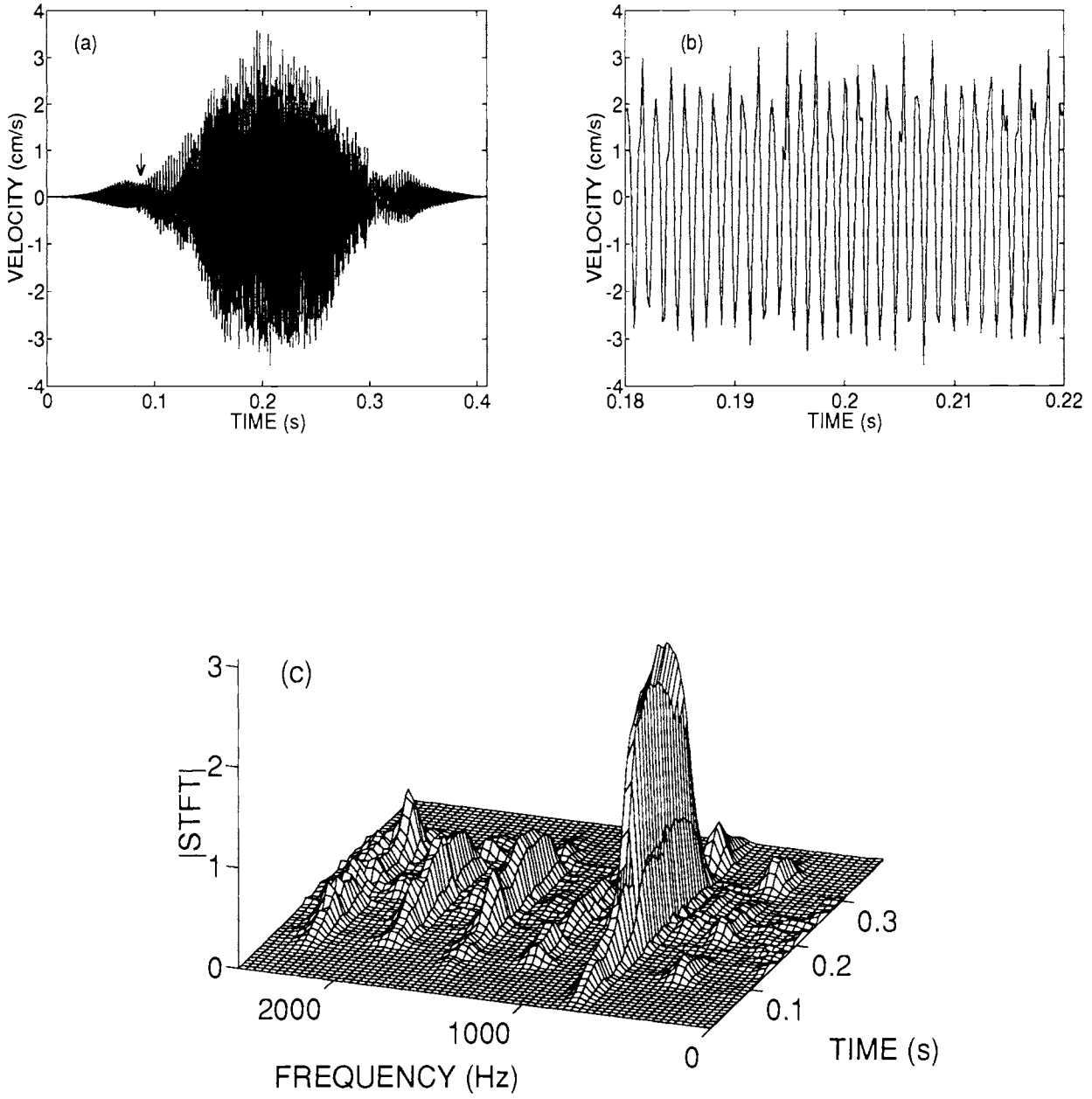

Figure 5: Velocity response of the same outer hair cell as in Fig. 4, but now to an AM stimulus with a carrier frequency of 756 Hz (at CF) and a modulation frequency of 2.44 Hz. The highest sound pressure level, occurring at the center of the input envelope, was 104 dB re .0002 dynes/cm^2. (a) Time waveform of the velocity response (in cm/s) of the cell. The time waveform does not follow the envelope of the stimulus, but undergoes a transition from a regular-like appearance to a more disordered appearance at times t = 0.9 s and t = 0.33 s. (b) Detailed view of the time waveform in the central region of the input envelope (from 0.18 s to 0.22 s). (c) Spectrogram of the velocity response shown in (a). The spectrogram shows spectral components at the carrier frequency f_c, and at two higher harmonic frequencies $2f_c$ and $3f_c$. In addition, components at the half-harmonic frequencies $f_c/2$, $3f_c/2$ and $5f_c/2$ are clearly visible in the time range 0.1 - 0.35 s, though these components do not follow the envelope of the input stimulus. There is also an overall raising of the noise-floor in the same time range, indicating a broadening of the spectral response away from frequencies related to the carrier frequency.

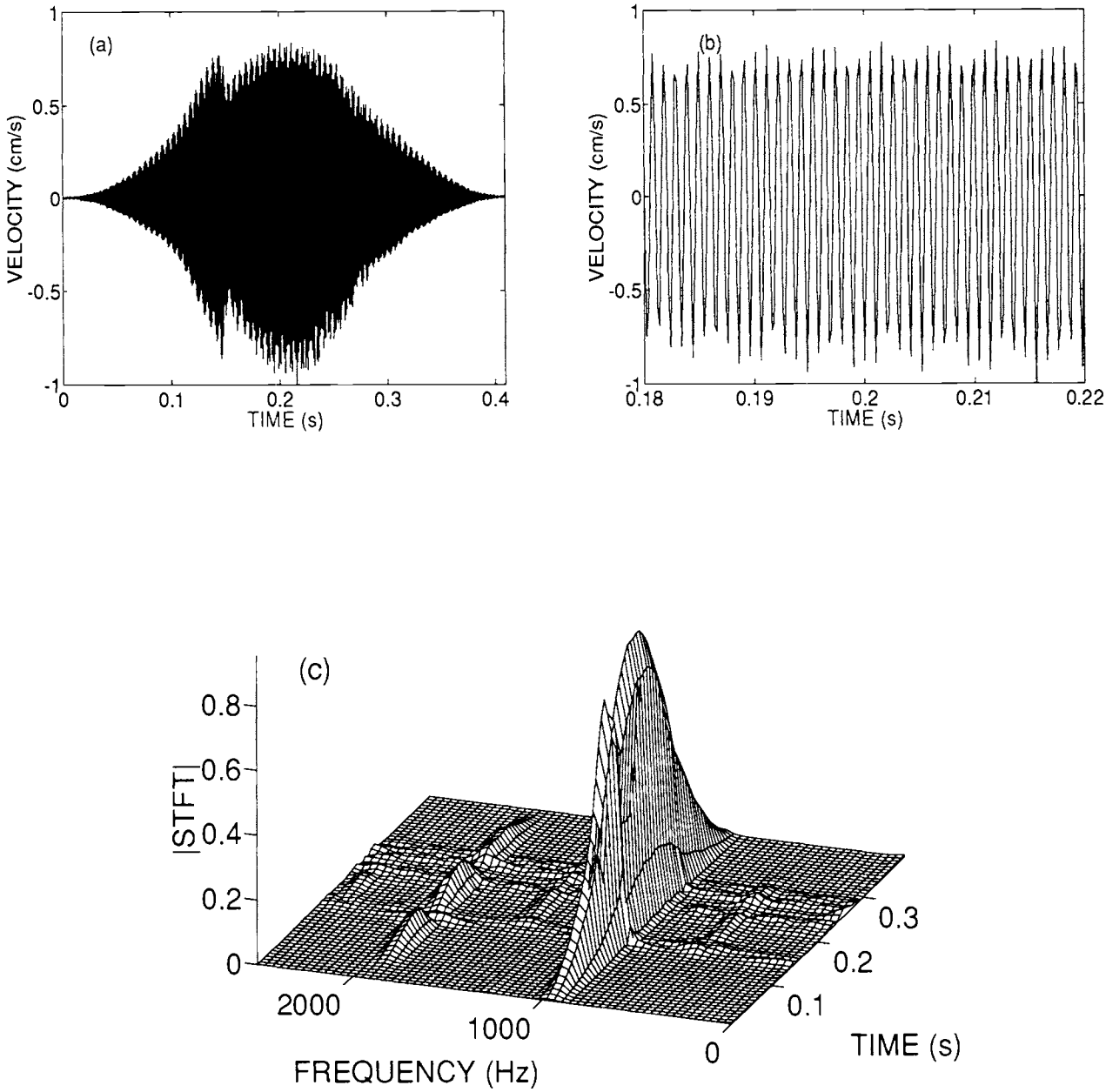

Figure 6: Velocity response of the same outer hair cell as in Figs. 4 and 5, but now to an AM stimulus with a carrier frequency of 961 Hz (just above CF) and a modulation frequency of 2.44 Hz. The highest sound pressure level, occurring at the center of the input envelope, was 99 dB:re .0002 dynes/cm^2. (a) Time waveform of the velocity response (in cm/s) of the cell. The time waveform follows the envelope of the stimulus quite well, apart from one clear notch occurring at time t = 0.15 s. (b) Detailed view of the time waveform in the central region of the input envelope (from 0.18 s to 0.22 s). (c) Spectrogram of the velocity response shown in (a). The spectrogram shows spectral components at the carrier frequency f_c, and at the second harmonic. Residual components at $f_c/2$ and $3f_c/2$ are just visible. The dominant spectral component is that at the carrier frequency.

4.2. The driven Duffing oscillator as a primitive model of cochlear dynamics

In an attempt to characterize the nonlinear mechanism(s) responsible for the unusual behavior we detailed above and elsewhere[7,15,16,17,18,19,20], we have considered analogies to other well-studied nonlinear systems. Keilson *et al.*[22,23,24], have analyzed the responses of a class of bilinear oscillators, and compared the results with experimental findings.

Here we consider a driven modified Duffing oscillator model [25,26,27], whose equation of motion is given by

$$\ddot{x}(t) + \alpha\dot{x}(t) - \beta x(t) + \gamma x^3(t) = F(t), \tag{5}$$

where $x(t)$ is position; t is time; α, β, and γ are constants; $F(t)$ is an arbitrary forcing function of time; and the overdot indicates differentiation with respect to time. This equation represents an oscillatory system with two symmetric potential wells. Since the potential energy is a quartic function of position, this equation models the motion of a ball, subject to an arbitrary driving force, oscillating in two valleys separated by an energy barrier.

Small motions within either of these wells have a clearly defined characteristic frequency (CF), the value of which is determined by suitable choice of the parameters α, β, and γ. The driving function, $F(t)$, can be arbitrarily chosen. For comparison with the cellular velocity data considered here, we choose $F(t)$ to be a slowly modulated AM signal of the form $F(t) = F_0[1 - \cos(2\pi f_m t)]\sin(2\pi f_c t)$ where f_m and f_c are the modulation and carrier frequencies of the AM signal, respectively, and F_0 is a constant. The characteristic frequency of the (small-amplitude) velocity response for the system was set at 700, by choosing $\alpha = 473$, $\beta = 9.7 \times 10^6$, and $\gamma = 4.85 \times 10^6$.

Figure 7 shows the velocity response $\dot{x}$ for such a system driven by a 100% amplitude modulated signal with carrier frequency 700 and modulation frequency 2.44, and with $F_0 = 2.56 \times 10^6$. The velocity response time waveforms in Figs. 7(a) and (b) are nearly sinusoidal in appearance, and the overall envelope of the response follows the input stimulus moderately closely. However, a sudden irregularity is visible in the time waveform at time $t = 0.22$. The spectrogram [Fig. 7(c)] of this velocity response, gives more information about the nature of this irregularity. The spectrogram shows spectral components at f_c, $2f_c$, and $3f_c$ which follow the input stimulus. However in the vicinity of time $t = 0.22$, spectral components at $f_c/2$, $3f_c/2$, and $5f_c/2$ briefly appear. This is a direct consequence of the sub-harmonic cascade (period-doubling[21]) route to chaos that the Duffing oscillator system is known to exhibit; as the magnitude of the driving force increases, the system is pushed toward chaotic behavior. This transition towards chaos is also accompanied by spectral broadening. These features resemble some of those observed in the cellular vibration data[19,20].

The Duffing oscillator itself does not seem destined to serve as a model for cellular dynamics in the cochlea; it is clearly too simple, too idealized, and not grounded in established physiology. Nevertheless some features of its behavior, such as the presence of half-harmonic spectral components and spectral broadening at high acoustic intensities, suggest that a reasonable model of cochlear dynamics may well contain a few of the elements of the Duffing system. But, then again, many other nonlinear systems with quite different characteristics also have these features. More work is clearly needed on the road toward identifying the character of the underlying nonlinearities in the cochlea.

5. ACKNOWLEDGMENTS

This work was supported by the Office of Naval Research under Grant N00014-92-J-1251, by the National Institutes of Health through NIDCD Program Project Grant DC00316, by the Emil Capita Foundation, by the Swedish Medical Research Council (02461), by the Magnus Bergvall Foundation, and by the Tysta Skolan Foundation.

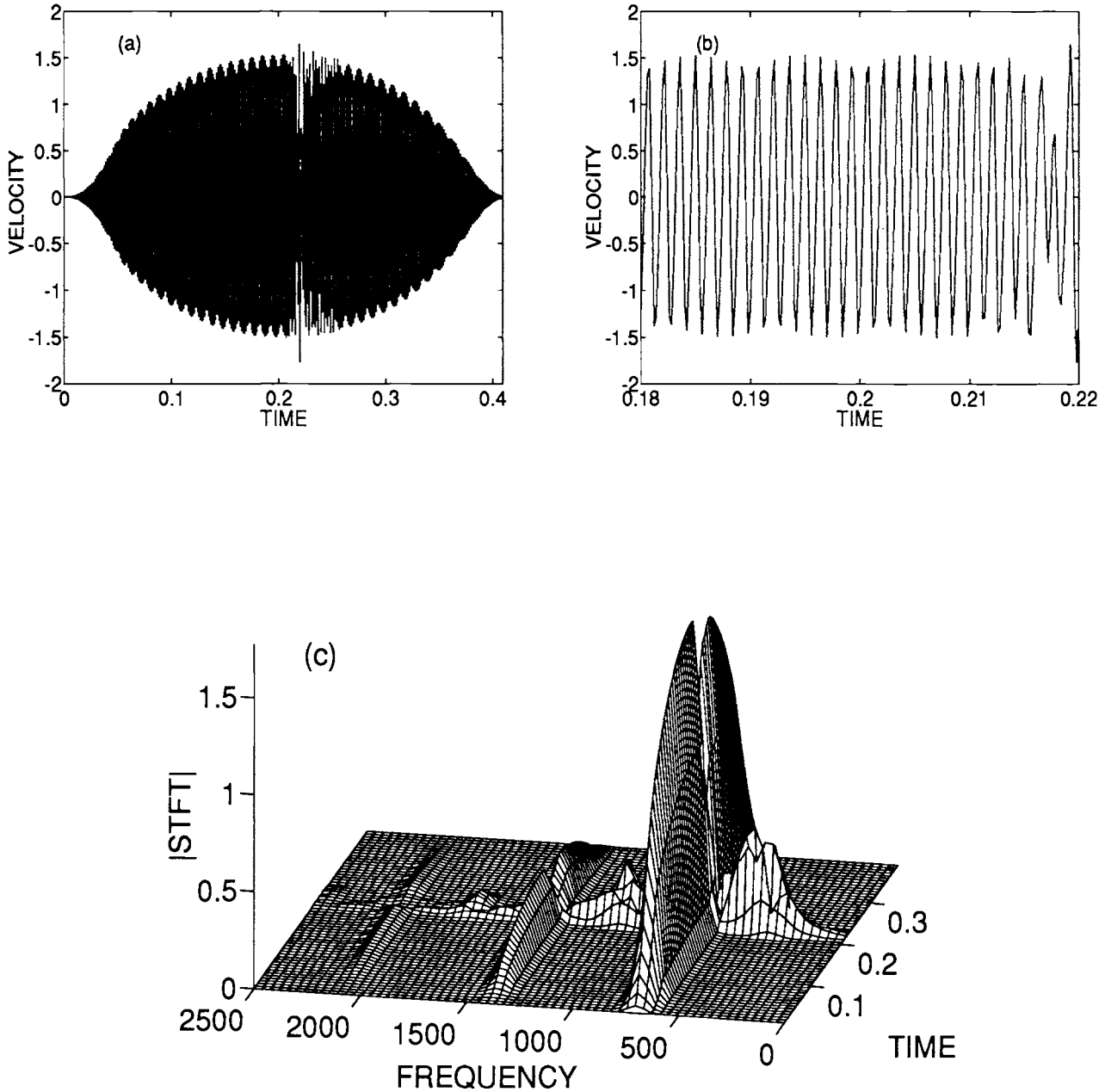

Figure 7: Velocity response of a model system based on the Duffing oscillator to an AM stimulus with a carrier frequency of 700 (at CF) and a modulation frequency of 2.44. (a) Time waveform of the velocity response of the model. The response follows the input stimulus envelope reasonably well. (b) Detailed view of the time waveform at the center of the input envelope (from 0.18 to 0.22). (c) Spectrogram of the velocity response shown in (a). At the center of the envelope, components at the half-harmonic frequencies $f_c/2$, $3f_c/2$, and $5f_c/2$ appear briefly. Some spectral broadening in the response is also apparent at that time. The harmonic components at $2f_c$ and $3f_c$ follow the shape of the input stimulus, in a similar way as the component at the carrier frequency.

6. REFERENCES

1. G. von Békésy, *Experiments in Hearing,* McGraw-Hill, New York, 1960.

2. J. O. Pickles, *An Introduction to the Physiology of Hearing,* Academic Press, New York, 1982.

3. E. F. Evans, "Functional anatomy of the auditory system," in *The Senses,* ed. H. B. Barlow and J. D. Mollon, pp. 251–306, Cambridge University Press, Cambridge, 1982.

4. W. S. Rhode and L. Robles, "Evidence from Mössbauer experiments for nonlinear vibration in the cochlea," *J. Acoust. Soc. Am.,* Vol. 55, pp. 588–596, March 1974.

5. E. LePage and B. M. Johnstone, "Nonlinear mechanical behavior of the basilar membrane in the basal turn of the guinea-pig cochlea," *Hearing Research,* Vol. 2, pp. 183–189, July 1980.

6. L. Robles, M. A. Ruggero, and N. C. Rich, "Basilar membrane mechanics at the base of the chinchilla cochlea. I. Input-output functions, tuning curves, and response phases," *J. Acoust. Soc. Am.,* Vol. 80, pp. 1364–1374, November 1986.

7. M. C. Teich, S. M. Khanna, and S. E. Keilson, "Nonlinear dynamics of cellular vibrations in the organ of Corti," *Acta Otolaryngologica (Stockholm),* Supplement 467, pp. 265-279, December 1989.

8. International Team for Ear Research (ITER), " Cellular vibration and motility in the organ of Corti," *Acta Otolaryngologica (Stockholm),* Supplement 467, pp. 1–279, December 1989.

9. M. Ulfendahl, Å. Flock, and S. M. Khanna, "A temporal bone preparation for the study of cochlear micromechanics at the cellular level," *Hearing Research,* Vol. 40, pp. 55–64, June 1989.

10. R. Franke, A. Dancer, S. M. Khanna, and M. Ulfendahl, "Intracochlear and extracochlear pressure measurements in the temporal-bone preparation of the guinea-pig," *Acustica,* Vol. 76, pp. 173–182, May 1992.

11. A. V. Oppenheim and R. W. Schafer, *Discrete-Time Signal Processing,* pp. 713–726, Prentice-Hall, Englewood Cliffs, NJ, 1989.

12. F. Hlawatsch and G. F. Boudreaux-Bartels, "Linear and quadratic time-frequency signal representations," *IEEE Signal Processing Magazine,* Vol. 9, No. 2, pp. 21–67, April 1992.

13. S. E. Keilson, S. M. Khanna, M. Ulfendahl, and M. C. Teich, "Spontaneous cellular vibrations in the guinea-pig cochlea," *Acta Otolaryngologica (Stockholm),* Vol. 113, pp. 591–597, September 1993.

14. S. M. Khanna, S. E. Keilson, M. Ulfendahl, and M. C. Teich, "Spontaneous cellular vibrations in the guinea-pig temporal-bone preparation," *British Journal of Audiology,* Vol. 27, 1993, in press.

15. S. E. Keilson, M. C. Teich, S. M. Khanna, and M. Ulfendahl, "The effect of sinusoidal stimuli on the spontaneous cellular vibrations in the guinea-pig cochlea," in *Abstracts of the Sixteenth Midwinter Research Meeting of the Association for Research in Otolaryngology,* ISSN 0742-3152, Abstract No. 336, p. 84, February 1993.

16. C. Heneghan, M. C. Teich, S. M. Khanna, M. Ulfendahl, L. Brundin, and Å. Flock, "Time-frequency representations of the dynamical motion of cellular structures in the organ of Corti," in *Abstracts of the Sixteenth Midwinter Research Meeting of the Association for Research in Otolaryngology,* ISSN 0742-3152, Abstract No. 338, p. 85, February 1993.

17. C. Heneghan, S. M. Khanna, Å. Flock, M. Ulfendahl, L. Brundin, and M. C. Teich, "Investigating the nonlinear dynamics of cellular motion in the inner ear using the spectrogram and the continuous wavelet transform," submitted for publication, 1993.

18. M. C. Teich, C. Heneghan, S. M. Khanna, Å. Flock, L. Brundin, and M. Ulfendahl, "Analysis of dynamical motion of sensory cells in the organ of Corti using the spectrogram," in *Biophysics of Hair Cell Sensory Systems,* ed. H. Duifhuis, J. W. Horst, P. van Dijk, and S. van Netten, World Scientific, Singapore, 1993, in press.

19. M. C. Teich, S. E. Keilson, S. M. Khanna, L. Brundin, M. Ulfendahl, and Å. Flock, "Chaos in the cochlea," in *Abstracts of the Fourteenth Midwinter Research Meeting of the Association for Research in Otolaryngology,* ISSN 0742-3152, Abstract No. 155, p. 50, February 1991.

20. M. C. Teich, S. E. Keilson, L. Brundin, M. Ulfendahl, and Å. Flock, "Chaotic vibrations of outer hair cells and Hensen's cells in the cochlea," in *Abstracts of the Fifteenth Midwinter Research Meeting of the Association for Research in Otolaryngology,* ISSN 0742-3152, Abstract No. 41, p. 17, February 1992.

21. P. Bergé, Y. Pomeau, and C. Vidal, *Order within Chaos,* pp. 210–220, Wiley-Interscience, New York, 1986.

22. S. E. Keilson, M. C. Teich, and S. M. Khanna, "Models of nonlinear vibration. I. Oscillator with bilinear resistance," *Acta Otolaryngologica (Stockholm),* Supplement 467, pp. 241–248, 1989.

23. M. C. Teich, S. E. Keilson, and S. M. Khanna, "Models of nonlinear vibration. II. Oscillator with bilinear stiffness," *Acta Otolaryngologica (Stockholm),* Supplement 467, pp. 249–256, 1989.

24. S. E. Keilson, M. C. Teich, and S. M. Khanna, "Models of nonlinear vibration. III. Oscillator with bilinear mass," *Acta Otolaryngologica (Stockholm)*, Supplement 467, pp. 257–264, 1989.

25. A. H. Nayfeh and D. T. Mook, *Nonlinear Oscillations*, pp. 161–224, Wiley-Interscience, New York, 1979.

26. S. De Souza-Machado, R. W. Rollins, D. T. Jacobs, and J. L. Hartman, "Studying chaotic systems using microcomputer simulations and Lyapunov exponents," *Am. J. Phys.*, Vol. 58, pp. 321–329, April 1990.

27. J.-C. Bacri, U. d'Ortona, and D. Salin, "Magnetic-fluid oscillator: observation of nonlinear period doubling," *Phys. Rev. Lett.*, Vol. 67, pp. 50–53, July 1991.